spectra of anhydrous nitrato complexes as the hydrogen-bonding arrangements change. In most other cases, however, it is difficult to detect the absorptions of the $O^{-}\cdots H^{+}$—N system as absorption from solvated molecules (H_2O or EtOH) interferes.

References

ADDISON, C. C., LOGAN, N., WALLWORK, S. C. & GARNER, C. D. (1971). *Q. Rev. Chem. Soc.* **25**, 289–322.

BULLOCK, J. I. (1967). *J. Inorg. Nucl. Chem.* **29**, 2257–2264.

BULLOCK, J. I. & TAJMIR-RIAHI, H.-A. (1977). *J. Chem. Soc. Dalton Trans.* pp. 36–39.

CALLIGARIS, M., NARDIN, G. & RANDACCIO, L. (1971). *Coord. Chem. Rev.* **7**, 385–403.

CAMERON, A. F., FORREST, K. P., TAYLOR, D. W. & NUTTALL, R. H. (1971). *J. Chem. Soc. A*, pp. 2492–2496.

CONDORELLI, G., FRAGALA, I., GUIFFRIDA, S. & CASSOL, A. (1975). *Z. Anorg. Allg. Chem.* **412**, 251–257.

DE BOLSTER, M. W. G. & GROENEVELD, W. L. (1971). *Recl Trav. Chim. Pays-Bas*, **90**, 477–507.

HOPPE, W. (1965). *Angew. Chem.* **77**, 484–492.

HVOSLEF, J. & KJELLEVOLD, K. E. (1974). *Acta Cryst.* B**30**, 2711–2716.

MAZHAR-UL-HAQUE, HART, F. A. & CAUGHLAN, C. N. (1970). *Chem. Commun.* pp. 1240–1241.

PAHOR, N. B., CALLIGARIS, M., DELISE, P., DODIC, G., NARDIN, G. & RANDACCIO, L. (1976). *J. Chem. Soc. Dalton Trans.* pp. 2478–2483.

RIBÁR, B., DIVJAKOVIĆ, V., HERAK, R. & PRELESNIK, B. (1973). *Acta Cryst.* B**29**, 1546–1548.

SANDORFY, C. (1970). *The Chemistry of the Carbon–Nitrogen Double Bond*, edited by S. PATAI, p. 42. New York: Interscience.

Acta Cryst. (1979). B**35**, 2020–2032

The Structure of Triclinic Ferrocene at 101, 123 and 148 K

BY PAUL SEILER AND JACK D. DUNITZ

Organic Chemistry Laboratory, Swiss Federal Institute of Technology, CH-8092 Zürich, Switzerland

(*Received* 16 *March* 1979; *accepted* 9 *May* 1979)

Abstract

X-ray diffraction patterns of the low-temperature triclinic modification of ferrocene were recorded from crystals cooled through the transition point at 164 K and also from a single crystal grown below 164 K by sublimation in an evacuated capillary tube, one end of which was warmed, the other cooled by a stream of nitrogen. The diffraction patterns can be indexed in terms of an *F*-centred triclinic cell with $a = 20{\cdot}960\ (8)$, $b = 15{\cdot}019\ (6)$, $c = 11{\cdot}421\ (5)$ Å, $\alpha = 89{\cdot}47\ (3)$, $\beta = 119{\cdot}93\ (3)$, $\gamma = 90{\cdot}62\ (3)°$ (at 101 K), $Z = 16$, where the axial orientation is chosen to correspond to the $P2_1/a$ orientation of the room-temperature monoclinic cell. If the centrosymmetric space group $F\bar{1}$ is assumed, the asymmetric unit consists of two $Fe(C_5H_5)_2$ molecules. Structure analyses were made with data collected at 101, 123 and 148 K. The two $Fe(C_5H_5)_2$ molecules have almost regular pentagonal cyclopentadienyl rings and show virtual D_5 symmetry (Fe–C 2·052, C–C 1·433 Å), the rings being mutually rotated by about 9° from the eclipsed orientation. Some aspects of the thermal-motion analysis, of the crystal packing, and of *X–X* deformation syntheses are discussed.

0567-7408/79/092020-13$01.00

Introduction

Ferrocene [bis(cyclopentadienyl)iron] undergoes a phase transition at 164 K (Edwards, Kington & Mason, 1960). The monoclinic high-temperature (HT) phase (space group $P2_1/a$, $Z = 2$) is disordered, and the nature of this disorder has only recently been clarified by X-ray and neutron diffraction studies at temperatures above and below the transition point (Seiler & Dunitz, 1979; Takusagawa & Koetzle, 1979). These studies show that the centrosymmetric structure formerly assigned to the ferrocene molecule in the crystalline state (Dunitz & Orgel, 1953; Dunitz, Orgel & Rich, 1956) is incorrect. As a consequence of the crystal disorder, individual ferrocene molecules need not have the molecular inversion centres that would be required by the space-group symmetry in an ordered structure; indeed, the new interpretations of both electron and nuclear scattering distributions in terms of superposition structures led to the conclusion that the conformation of the ferrocene molecules in the crystal was neither staggered (D_{5d}) nor eclipsed (D_{5h}) but intermediate (D_5).

In our earlier paper (Seiler & Dunitz, 1979) we drew on some results of a preliminary analysis of the low-

temperature (LT) phase, the structure of which was previously unknown. In the present paper we present results on the structure of ferrocene at three temperatures (101, 123, 148 K) below the transition point.

Crystal data

At temperatures below 164 K the unit translations along all three crystal axes of the monoclinic HT cell are doubled (Table 1). To avoid confusion, reflexion indices referred to the HT cell are written as h, k, l, those referred to the LT cell as H, K, L. Apart from a few very weak reflexions produced by some crystal specimens, the observed reflexions satisfy the condition that H, K, L are either all even or all odd. The LT cell is therefore face-centred, at least in good approximation. Reflexions with H, K, L even are common to both phases ($H = 2h$, $K = 2k$, $L = 2l$) and have approximately the same intensity in both. However, the glide planes and screw axes of the monoclinic HT space group are obviously incompatible with the doubling of the cell axes. Hence the LT structure must be triclinic. For simplicity we assume that the cell is face-centred and centrosymmetric: space group $F\bar{1}$.

Experimental

Lattice dimensions and diffracted intensities were measured with an Enraf–Nonius CAD-4 diffractometer (Mo $K\alpha$ radiation, $\lambda = 0{\cdot}71069$ Å) equipped with a graphite monochromator and a slightly modified Nonius low-temperature device.

Crystals of ferrocene are reported to disintegrate, sometimes violently, on cooling to temperatures below the transition point (Bodenheimer & Low, 1971). We experienced no difficulties on this score because we took the precaution of embedding our crystal specimens in epoxy resin. The main source of difficulty was that the triclinic crystals produced by cooling through the transition point tended to form as twinned intergrowths showing considerable mosaic spread in their X-ray diffraction patterns. Typical reflexion profiles from crystals of the LT phase were 2–5° in width, about five times wider than those of corresponding reflexions from the monoclinic phase. On rewarming individual specimens slowly to room temperature (RT) the original crystal quality was partially restored, but repeated passage through the phase transition led to a noticeable deterioration in crystal quality.

Table 1. *Lattice dimensions of ferrocene at five temperatures*

The directions of **a** and **c** are reversed with respect to the cell described by Calvarin & Bérar (1975).

E.s.d.'s are about 0·04% in lengths and 0·03° in angles.

	101 K	123 K	148 K	173 K	293 K
a (Å)	20·960	20·973	20·969	10·449	10·535
b (Å)	15·019	15·037	15·066	7·579	7·611
c (Å)	11·421	11·454	11·501	5·814	5·929
α (°)	89·47	89·52	89·61	90	90
β (°)	119·93	120·03	120·16	120·86	121·03
γ (°)	90·62	90·58	90·48	90	90
V (Å^3)	3116	3127	3141	395·2	407·4
Space group	$F\bar{1}$	$F\bar{1}$	$F\bar{1}$	$P2_1/a$	$P2_1/a$

Because of the closeness of the interaxial angles α and γ to 90° and the large mosaic spread, HKL and $H\bar{K}L$ reflexions from individual twin components were virtually superimposed. The interaxial angles could be estimated from the splitting of high-order peaks, but it was not possible to measure $I(HKL)$ and $I(H\bar{K}L)$ separately, only their weighted sum. As the analysis progressed, an approximate twinning correction could be estimated (see below), but it also became evident that although the twinned intensity data could furnish a rough description of the crystal structure they were inadequate to determine atomic positions and vibrational parameters with the desired degree of accuracy.

At this stage we began to consider ways of obtaining untwinned crystals of the triclinic LT phase. It was clear that attempts to produce untwinned crystals by cooling from the HT phase were unlikely to meet with success. As the temperature is lowered the monoclinic → triclinic transition is presumably initiated by the formation of small triclinic regions that then grow, on further cooling, into the surrounding crystal. Insofar as the domains first formed are separate, each can be expected to occur at random in either of the two possible orientations related by reflexion across the (010) plane of the monoclinic crystal. At any rate, every crystal we obtained by cooling through the transition point turned out to be twinned.

We then considered the possibility of circumventing the phase transition by growing a single crystal of the triclinic phase from the vapour at a temperature below 164 K. The vapour pressure of ferrocene is 9×10^{-1} Pa at RT and reaches a value of 10^2 Pa only at 360 K (Edwards & Kington, 1962); extrapolation to lower temperature gives a value of about 10^{-11} Pa at 160 K. A device was constructed whereby a small sample of material at one end of an evacuated capillary could be heated by an electric coil while the other end of the capillary (about 10 mm in length) was cooled by a fine stream of cold nitrogen. The entire device, details of which will be described elsewhere, was mounted on the diffractometer so that the crystal-growth process could be observed through the telescope and diffraction measurements could be carried out without warming or disturbing the crystal once it had formed. After many

frustrations caused by expected and unexpected difficulties it was possible to grow a single untwinned crystal of triclinic ferrocene and measure its diffraction pattern.

Although the crystal obtained by this method was small and did not show well developed faces, its crystal quality, as judged by the mosaic spread, was almost as good as that of the RT crystals.

There is a marked difference in colour between the two phases; the monoclinic crystals change from deep orange at RT to light orange at about 170 K, and the triclinic ones are lemon coloured, becoming more greenish than yellowish as the temperature is lowered.

Structure analysis and refinement

We first describe results based on measurements from a twinned crystal obtained by cooling through the phase transition. Intensities were measured for about 12 700 reflexions at 100 K ($\sin\theta/\lambda$ limit = 1·0 Å^{-1}, about 7600 reflexions with $I > 2{\cdot}5\sigma_I$) and converted to relative F values in the usual way.

A preliminary least-squares refinement was made using only reflexions with H, K, L all even (those common to the triclinic and monoclinic structures). These reflexions correspond to a superposition electron density that can be described in terms of a model consisting of an Fe atom situated on one of the inversion centres of the monoclinic structure and 20 half-weight C atoms (10 per asymmetric unit). The C atoms were assigned isotropic temperature factors, the Fe atom an anisotropic one. It was the interpretation of the results of this refinement that first led us to the conclusion that the ferrocene molecules in the LT phase were not centrosymmetric (for more extended discussion of this point see Seiler & Dunitz, 1979). More important in the present context is the prominent anisotropy found for the Fe atom in the superposition structure. This anisotropy was obviously to be interpreted not as genuine thermal motion but as an indication that individual Fe atoms were displaced from the assumed inversion centres of the model structure.* The direction and magnitude of these displacements could be estimated from the shape of the Fe vibrational ellipsoid. This information provided a starting-point for a least-squares refinement of the Fe positions in the lower space group, utilizing all reflexions with $I > 10\sigma_I$ [two independent Fe atoms, isotropic, modified weighting scheme with $r = 2{\cdot}5$ Å^2 (Dunitz & Seiler, 1973)] and leading to $R = 0{\cdot}28$.

A heavy-atom F_o Fourier synthesis calculated at this stage showed around each of the two symmetry-independent heavy-atom peaks a group of 10 prominent peaks arranged in the form of a pair of parallel five-membered rings. A second group of 20 somewhat weaker peaks (0·5–0·7 ratio of peak heights) was related to the first group by reflexion across the plane $y = 0$. The occurrence of these additional peaks was attributed partly to the pseudo-hypercentric nature of the Fe arrangement and partly to the effect of twinning in the experimental F values. These peaks were therefore regarded as being spurious and were ignored in the derivation of the model for the subsequent least-squares analysis, which converged at $R = 0{\cdot}12$ (Fe and C atoms anisotropic, H atoms ignored) for the 7600 reflexions with $I > 2{\cdot}5\sigma_I$. The resulting structural model consisted of two nearly identical ferrocene molecules that were neither staggered nor eclipsed, but rotated by about 9° from the latter. The 20 symmetry-independent Fe···C distances varied between 2·00 and 2·08 Å, the C–C distances between 1·40 and 1·46 Å.

By comparing I_o and I_c values for several pairs of HKL and $H\bar{K}L$ reflexions, the ratio of the twin components was estimated to be approximately 2 : 1 (in rough agreement with an estimate based on the ratio of major to minor peak heights in the F_o Fourier synthesis). Our intensity data included about 2210 reflexion pairs with $I > 6\sigma_I$ for both members of the pair; the twinning correction was applied to these reflexions. The least-squares analysis was then resumed with this subset of reflexions, leading to convergence at $R = 0{\cdot}08$. The resulting structural model showed somewhat more regular geometry than before, but it was not at all clear to what extent the remaining irregularities (Fe–C 2·03–2·06 Å, C–C 1·41–1·44 Å) were real or due to the inadequacy of the twinning correction or other insufficiencies in the experimental data. We were particularly worried about the large difference between the vibrational tensors obtained for the two Fe atoms; the major axis of the vibrational ellipsoid pointed in one case nearly along the molecular fivefold axis, in the other nearly at right angles to this axis.

We turn now to the results obtained with an untwinned crystal, which was produced as described in *Experimental*. The crystal in question was of irregular shape with mean diameter ~0·16 mm. Intensity measurements were made at three temperatures below the transition point: 101 K ($\sin\theta/\lambda$ limit 0·66 Å^{-1}, 2969 reflexions with $I > 3\sigma_I$); 123 K ($\sin\theta/\lambda$ limit 0·60 Å^{-1}, 2183 reflexions with $I > 3\sigma_I$); and 148 K (2171 reflexions with $I > 3\sigma_I$). All three data sets were refined by least squares. With the 101 K data, convergence was reached at $R = 0{\cdot}057$ (Fe and C isotropic, H atoms omitted), at $R = 0{\cdot}035$ (Fe and C anisotropic, H atoms omitted) and finally at $R = 0{\cdot}019$ (isotropic H atoms, extinction correction, modified weighting scheme with $r = 2{\cdot}5$ Å^2). For the two other data sets final convergence was reached at $R = 0{\cdot}020$ (123 K)

* The displacements in question are indicated schematically by the arrows associated with the molecular centres in Fig. 3 of Seiler & Dunitz (1979).

Table 2. *Positional coordinates* ($\times 10^5$ *for* Fe *and* C *atoms*; $\times 10^4$ *for* H *atoms*) *with e.s.d.'s in parentheses*

For each atom the result of the 101 K analysis (top line of values) is followed by results of the 123 K and 148 K analyses.

	Molecule (I)				Molecule (II)		
	x	*y*	*z*		*x*	*y*	*z*
Fe	25206 (1)	−562 (1)	374 (2)	Fe	878 (1)	24935 (1)	815 (2)
	25204 (1)	−545 (2)	375 (3)		845 (1)	24948 (2)	777 (3)
	25197 (1)	−512 (2)	366 (3)		789 (1)	24964 (2)	716 (3)
C(1)	27415 (8)	12769 (9)	3314 (20)	C(1)	2547 (8)	11538 (9)	3598 (18)
	27389 (12)	12742 (14)	3248 (29)		2551 (11)	11611 (13)	3499 (26)
	27360 (14)	12732 (15)	3165 (34)		2497 (12)	11695 (14)	3281 (30)
C(2)	26259 (8)	10188 (11)	−9574 (19)	C(2)	1849 (8)	14166 (10)	−9006 (17)
	26275 (12)	10159 (15)	−9518 (26)		1872 (11)	14241 (14)	−9013 (24)
	26298 (13)	10117 (17)	−9515 (30)		1864 (12)	14349 (16)	−9063 (27)
C(3)	31614 (8)	3642 (10)	−7494 (16)	C(3)	7501 (8)	20544 (10)	−6402 (16)
	31616 (11)	3663 (14)	−7374 (23)		7495 (11)	20571 (14)	−6328 (22)
	31662 (13)	3658 (17)	−7208 (27)		7514 (12)	20665 (15)	−6259 (25)
C(4)	36040 (7)	2203 (10)	6633 (16)	C(4)	11680 (7)	21815 (10)	7819 (16)
	36015 (10)	2288 (14)	6650 (22)		11637 (10)	21782 (14)	7822 (22)
	36004 (11)	2339 (15)	6752 (25)		11601 (11)	21833 (15)	7795 (25)
C(5)	33454 (8)	7803 (10)	13368 (16)	C(5)	8653 (7)	16269 (10)	14041 (16)
	33425 (11)	7829 (14)	13270 (22)		8608 (10)	16302 (14)	13893 (21)
	33407 (12)	7869 (16)	13256 (26)		8538 (12)	16316 (16)	13750 (24)
C(6)	16518 (7)	−3176 (9)	3386 (16)	C(6)	−7966 (7)	27763 (10)	3061 (18)
	16532 (10)	−3191 (13)	3367 (22)		−7986 (11)	27816 (14)	3043 (24)
	16544 (11)	−3188 (14)	3319 (25)		−8044 (12)	27810 (15)	2996 (28)
C(7)	14485 (7)	−4814 (10)	−10277 (16)	C(7)	−9630 (8)	29524 (11)	−10427 (18)
	14508 (10)	−4821 (14)	−10218 (23)		−9649 (11)	29538 (15)	−10371 (25)
	14500 (11)	−4760 (16)	−10192 (26)		−9719 (13)	29510 (17)	−10297 (29)
C(8)	19293 (8)	−11445 (10)	−10417 (16)	C(8)	−4522 (9)	35992 (10)	−10073 (17)
	19278 (12)	−11405 (14)	−10406 (22)		−4603 (13)	35959 (15)	−10047 (24)
	19272 (13)	−11326 (16)	−10444 (25)		−4714 (15)	35953 (16)	−10048 (27)
C(9)	24302 (7)	−13872 (9)	3249 (16)	C(9)	338 (8)	38278 (9)	3732 (17)
	24282 (11)	−13806 (13)	3231 (22)		268 (11)	38264 (13)	3730 (23)
	24296 (12)	−13773 (14)	3127 (25)		185 (13)	38236 (14)	3669 (26)
C(10)	22598 (7)	−8803 (9)	11808 (15)	C(10)	−1804 (7)	33180 (9)	11847 (16)
	22584 (10)	−8791 (13)	11709 (21)		−1848 (11)	33162 (13)	11740 (22)
	22605 (11)	−8772 (14)	11648 (23)		−1872 (12)	33180 (14)	11677 (25)
H(1)	2449 (12)	1744 (15)	498 (25)	H(1)	−89 (11)	692 (14)	513 (24)
	2476 (14)	1738 (17)	533 (28)		−111 (13)	720 (16)	513 (26)
	2488 (16)	1740 (20)	505 (33)		−124 (14)	715 (17)	509 (28)
H(2)	2198 (13)	1228 (16)	−1893 (26)	H(2)	−208 (13)	1180 (16)	−1814 (25)
	2213 (16)	1179 (19)	−1861 (32)		−194 (14)	1207 (17)	−1789 (28)
	2189 (19)	1165 (23)	−1895 (38)		−196 (15)	1221 (18)	−1798 (30)
H(3)	3184 (13)	16 (15)	−1472 (26)	H(3)	808 (11)	2348 (14)	−1331 (23)
	3203 (15)	15 (18)	−1420 (30)		805 (12)	2325 (15)	−1286 (25)
	3204 (17)	10 (20)	−1404 (33)		801 (14)	2336 (17)	−1303 (28)
H(4)	4028 (12)	−208 (16)	1110 (25)	H(4)	1601 (12)	2607 (15)	1257 (24)
	4012 (14)	−173 (17)	1077 (28)		1573 (13)	2596 (16)	1234 (26)
	4025 (15)	−174 (19)	1086 (31)		1575 (14)	2611 (18)	1255 (29)
H(5)	3546 (12)	832 (15)	2298 (25)	H(5)	1040 (12)	1566 (15)	2358 (23)
	3542 (13)	826 (17)	2254 (27)		1022 (12)	1594 (15)	2274 (23)
	3549 (17)	850 (20)	2255 (33)		1018 (13)	1601 (17)	2296 (26)
H(6)	1430 (12)	120 (15)	658 (25)	H(6)	−1056 (12)	2352 (16)	596 (25)
	1426 (13)	137 (16)	641 (25)		−1055 (13)	2406 (17)	543 (26)
	1430 (15)	133 (18)	670 (29)		−1055 (15)	2356 (19)	575 (30)
H(7)	1034 (13)	−201 (17)	−1827 (27)	H(7)	−1339 (13)	2656 (16)	−1885 (26)
	1055 (14)	−240 (18)	−1786 (28)		−1316 (15)	2663 (19)	−1865 (30)
	1062 (16)	−233 (20)	−1755 (33)		−1330 (17)	2662 (21)	−1834 (33)
H(8)	1902 (12)	−1412 (15)	−1885 (24)	H(8)	−446 (12)	3813 (15)	−1790 (25)
	1927 (13)	−1382 (16)	−1838 (27)		−451 (14)	3772 (17)	−1730 (28)
	1920 (14)	−1388 (17)	−1863 (28)		−465 (17)	3770 (20)	−1790 (33)
H(9)	2815 (12)	−1840 (14)	644 (23)	H(9)	460 (11)	4258 (14)	721 (23)
	2798 (12)	−1827 (15)	623 (25)		462 (12)	4265 (15)	716 (24)
	2782 (14)	−1831 (17)	613 (28)		464 (13)	4265 (16)	717 (26)
H(10)	2538 (11)	−873 (13)	2189 (22)	H(10)	56 (11)	3282 (13)	2148 (22)
	2525 (12)	−855 (14)	2151 (24)		50 (11)	3272 (14)	2099 (23)
	2539 (13)	−849 (16)	2167 (27)		59 (12)	3266 (15)	2129 (25)

Table 3. *Vibration parameters* (Å²) (*all* $\times 10^3$ *with e.s.d.'s in parentheses*) *for the results of the* 101 K (*top line*), 123 K (*middle line*) *and* 148 K (*bottom line*) *analyses*

	U_{11}	U_{22}	U_{33}	U_{12}	U_{13}	U_{23}	U (H)
Molecule (I)							
Fe	101 (1)	87 (1)	131 (1)	−11 (1)	60 (1)	−8 (1)	
	128 (1)	108 (1)	162 (1)	−15 (1)	76 (1)	−8 (1)	
	164 (1)	136 (1)	215 (2)	−20 (1)	98 (1)	−9 (1)	
C(1)	231 (6)	113 (6)	510 (11)	−31 (5)	229 (7)	−34 (6)	393 (40)
	287 (11)	142 (10)	684 (18)	−58 (8)	306 (12)	−64 (11)	493 (79)
	372 (13)	153 (11)	962 (24)	−66 (10)	423 (15)	−83 (13)	690 (101)
C(2)	199 (6)	221 (7)	338 (9)	−29 (5)	98 (6)	107 (6)	449 (43)
	263 (11)	284 (12)	403 (14)	−49 (9)	119 (10)	150 (10)	644 (93)
	342 (13)	343 (14)	530 (18)	−90 (11)	131 (12)	190 (13)	961 (125)
C(3)	237 (6)	240 (7)	226 (8)	−67 (5)	151 (6)	−19 (6)	404 (40)
	283 (10)	290 (12)	287 (12)	−100 (9)	193 (9)	−32 (9)	544 (84)
	380 (13)	382 (14)	371 (15)	−140 (11)	247 (12)	−47 (11)	731 (102)
C(4)	139 (5)	195 (6)	240 (7)	−21 (4)	106 (5)	−7 (5)	383 (39)
	170 (9)	232 (10)	312 (12)	−18 (8)	133 (9)	13 (9)	472 (77)
	220 (10)	276 (12)	410 (15)	−26 (9)	174 (10)	9 (10)	611 (91)
C(5)	205 (6)	226 (7)	246 (8)	−92 (5)	137 (6)	−80 (6)	371 (39)
	239 (10)	294 (11)	280 (12)	−139 (8)	158 (9)	−111 (9)	422 (74)
	315 (12)	362 (13)	373 (15)	−170 (10)	205 (11)	−122 (11)	714 (101)
C(6)	146 (5)	169 (6)	269 (8)	−6 (4)	118 (5)	−7 (5)	386 (40)
	189 (9)	196 (10)	338 (12)	−32 (8)	156 (9)	−18 (9)	374 (70)
	232 (10)	245 (11)	414 (15)	−39 (8)	186 (10)	−29 (10)	564 (88)
C(7)	146 (5)	208 (6)	216 (7)	−43 (5)	43 (5)	22 (5)	466 (44)
	162 (9)	261 (11)	265 (12)	−58 (8)	38 (8)	36 (9)	486 (79)
	209 (10)	317 (13)	350 (14)	−73 (9)	63 (10)	49 (10)	708 (102)
C(8)	244 (6)	185 (6)	189 (7)	−84 (5)	114 (5)	−61 (5)	335 (37)
	334 (11)	220 (10)	243 (12)	−133 (8)	160 (9)	−90 (9)	382 (71)
	442 (13)	281 (12)	302 (13)	−178 (10)	205 (11)	−120 (10)	469 (79)
C(9)	199 (6)	122 (5)	229 (7)	−12 (4)	120 (5)	−18 (5)	295 (35)
	237 (9)	143 (9)	295 (12)	−28 (7)	145 (9)	−14 (8)	318 (65)
	296 (11)	175 (10)	382 (14)	−29 (8)	200 (10)	−15 (9)	426 (75)
C(10)	171 (5)	158 (6)	176 (6)	−22 (4)	96 (5)	3 (5)	261 (33)
	211 (9)	206 (10)	202 (11)	−51 (8)	120 (8)	−6 (8)	273 (62)
	263 (10)	246 (11)	272 (12)	−60 (8)	160 (10)	0 (9)	385 (72)
Molecule (II)							
Fe	110 (1)	91 (1)	132 (1)	16 (1)	63 (1)	−3 (1)	
	138 (1)	111 (1)	161 (1)	20 (1)	76 (1)	−3 (1)	
	176 (1)	141 (1)	214 (2)	24 (1)	101 (1)	−4 (1)	
C(1)	202 (6)	116 (6)	382 (9)	17 (5)	175 (6)	−5 (6)	302 (35)
	250 (10)	147 (10)	500 (15)	39 (8)	232 (10)	8 (9)	363 (68)
	328 (12)	169 (11)	692 (19)	57 (9)	327 (13)	17 (11)	452 (78)
C(2)	178 (6)	216 (7)	257 (8)	8 (5)	88 (5)	−108 (6)	397 (41)
	210 (10)	278 (12)	326 (13)	38 (8)	102 (9)	−137 (10)	466 (78)
	259 (11)	351 (13)	417 (16)	49 (10)	128 (11)	−184 (11)	553 (87)
C(3)	224 (6)	209 (6)	224 (7)	30 (5)	152 (6)	−8 (5)	272 (34)
	284 (10)	240 (11)	280 (12)	66 (8)	200 (9)	18 (9)	291 (63)
	349 (12)	294 (12)	358 (14)	80 (10)	251 (11)	23 (10)	479 (80)
C(4)	138 (5)	192 (6)	242 (7)	−1 (4)	102 (5)	−49 (5)	373 (39)
	160 (9)	235 (10)	311 (12)	7 (8)	118 (9)	−48 (9)	386 (70)
	199 (10)	279 (12)	385 (14)	13 (8)	150 (10)	−66 (10)	523 (84)
C(5)	183 (6)	221 (6)	202 (7)	76 (5)	102 (5)	32 (5)	297 (34)
	225 (9)	277 (11)	205 (11)	115 (8)	115 (9)	43 (9)	219 (55)
	290 (11)	363 (13)	289 (13)	150 (10)	167 (10)	70 (10)	348 (67)
C(6)	169 (6)	174 (6)	356 (9)	32 (5)	150 (6)	−10 (6)	390 (40)
	206 (9)	194 (10)	456 (14)	37 (8)	203 (10)	−13 (10)	407 (72)
	255 (11)	240 (12)	585 (18)	49 (9)	247 (12)	−5 (11)	595 (90)
C(7)	195 (6)	248 (7)	280 (8)	105 (5)	34 (6)	−34 (6)	435 (42)
	225 (10)	300 (12)	338 (13)	137 (9)	24 (9)	−51 (10)	587 (89)
	283 (12)	365 (14)	461 (17)	170 (11)	12 (12)	−93 (12)	729 (104)
C(8)	380 (8)	199 (7)	233 (8)	138 (6)	171 (6)	67 (6)	362 (38)
	468 (13)	245 (11)	286 (13)	201 (10)	207 (11)	106 (10)	470 (78)
	582 (16)	297 (13)	343 (15)	242 (12)	256 (13)	110 (11)	715 (102)
C(9)	268 (6)	123 (6)	281 (8)	29 (5)	188 (6)	4 (5)	266 (33)
	324 (11)	155 (9)	334 (12)	56 (8)	226 (10)	5 (9)	281 (61)
	408 (13)	179 (10)	411 (15)	64 (9)	275 (12)	2 (10)	361 (69)

Table 3 (*cont.*)

	U_{11}	U_{22}	U_{33}	U_{12}	U_{13}	U_{23}	U (H)
C(10)	215 (6)	156 (6)	230 (7)	43 (5)	149 (5)	4 (5)	264 (33)
	264 (10)	185 (10)	267 (12)	56 (8)	181 (9)	3 (8)	260 (60)
	329 (11)	232 (11)	345 (13)	60 (9)	236 (10)	−4 (10)	349 (69)

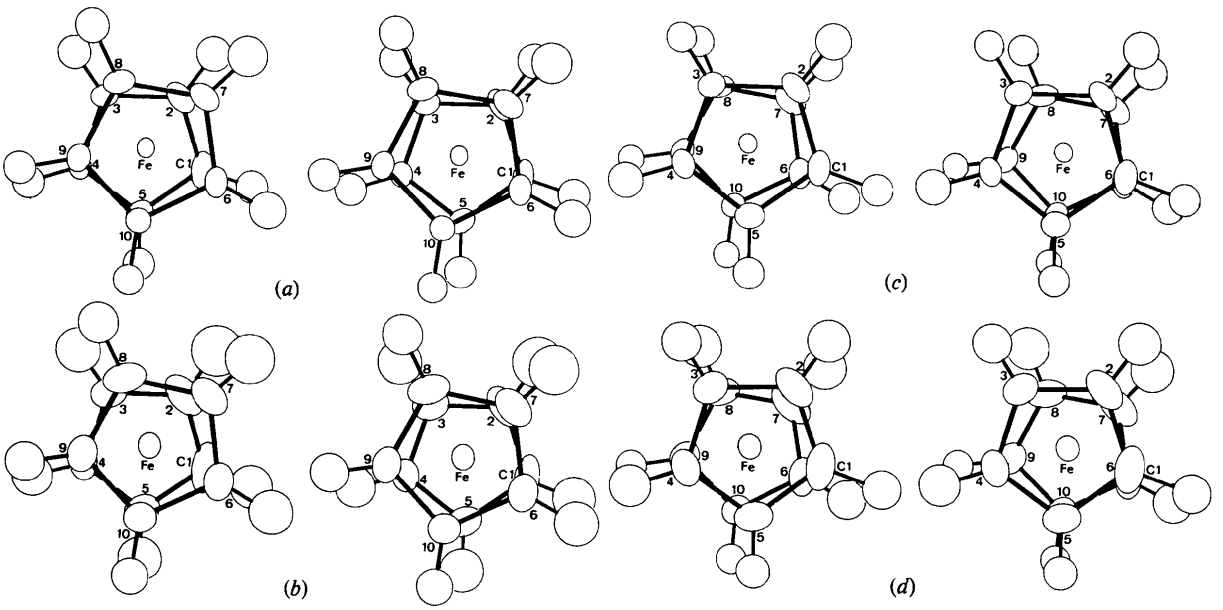

Fig. 1. Stereoscopic views of molecule (I) (*a*) at 101 K and (*b*) at 148 K, and of molecule (II) (*c*) at 101 K and (*d*) at 148 K. Vibrational ellipsoids, isotropic for H atoms, are shown at the 50% probability level (Johnson, 1965).

and at $R = 0{\cdot}021$ (148 K) with the same number and type of least-squares parameters. Absorption corrections were not applied ($\mu \sim 1{\cdot}9$ mm^{-1}) in view of the difficulty in measuring the irregular shape of the crystal, but the errors introduced by neglecting these corrections should be small. Standard scattering factors for neutral atoms were adopted (*International Tables for X-ray Crystallography*, 1968), dispersion corrections ($f' = 0{\cdot}4, f'' = 1{\cdot}0$) being ignored.

Positional coordinates obtained from the three analyses are given in Table 2, vibrational parameters in Table 3.*

Molecular geometry

In this section we shall concentrate on the results obtained in 101 K analysis since they are least affected by the effects of thermal motion and disorder.

The two independent molecules in the asymmetric unit of the crystal have virtually identical structures. As seen from Fig. 1, the molecules are neither eclipsed nor staggered, although somewhat closer to the former. If we define a rotation angle as being zero for eclipsed and 36° for staggered, it is 8·7 and 8·8° for molecules (I) and (II) respectively at 101 K, 8·9 and 9·2° at 123 K, and 9·5 and 9·9° at 148 K.

Increase in temperature is accompanied by a slight apparent shortening of the bond lengths, but this is practically nullified by thermal-motion corrections. Averaged Fe–C and C–C distances (corrected values in parentheses) obtained from the three analyses are (in Å):

	101 K	123 K	148 K
Fe–C	2·046 (2·052)	2·043 (2·051)	2·041 (2·052)
C–C	1·426 (1·433)	1·418 (1·428)	1·415 (1·430).

Even at 101 K the thermal-motion corrections are not negligible (see later). Table 4 shows that at 101 K individual Fe–C and C–C distances do not vary by more than 0·007 Å from their respective mean values. The cyclopentadienyl C-atom skeletons thus appear as almost perfectly regular pentagons whose vertices are

* Lists of structure factors measured at 101, 123 and 148 K have been deposited with the British Library Lending Division as Supplementary Publication No. SUP 34457 (24 pp.). Copies may be obtained through The Executive Secretary, International Union of Crystallography, 5 Abbey Square, Chester CH1 2HU, England.

equidistant from the Fe atom. At the higher temperature the scatter in the individual distances is slightly greater than at 101 K, but it is still within the range expected from the e.s.d.'s in positional parameters (Table 2). The Fe–C distances with corrected values in parentheses are 2·035 (2·044)–2·050 (2·057) Å at 123 K and 2·027 (2·039)–2·052 (2·061) Å at 148 K; the C–C distances are 1·410 (1·420)–1·429 (1·439) Å at 123 K and 1·406 (1·420)–1·424 (1·440) Å at 148 K. At all three temperatures the mean corrected Fe–C and C–C distances are slightly shorter than the corresponding distances obtained by electron diffraction of gaseous ferrocene at 413 K (Fe–C 2·064, C–C 1·440 Å; Haaland, 1975).

At 101 K each of the four cyclopentadienyl ring skeletons in the asymmetric unit is planar to within 0·002 Å, and each Fe atom lies within 0·005 Å of the centre of its mass-independent molecular inertial system. The angle between the two ring-planes in each molecule is 0·46° for molecule (I) and 0·74° for molecule (II). Disregarding these small deviations, we can say that the C-atom frameworks of both molecules have very nearly perfect D_5 symmetry in the crystal. The individual molecules are chiral. The assumed space group $F\bar{1}$ would require that there are equal numbers of enantiomers.

Apart from the systematic shortening of the C–H distances [mean value 1·00 Å (Table 4)], the H positions obtained from the refinement show a less regular arrangement than the C-atom skeletons. If the H atoms were exactly on the spokes of the pentagons, all H–C–C angles would be 126°. Of the 40 observed angles of this type (Table 5), nine deviate from 126° by more than 1·5° (~1σ), the maximum deviation being 2·8°. These deviations are thus well within the experimental uncertainties and could be dismissed from further consideration. However, they do show a systematic behaviour in that the nine largest angular deviations all occur in molecule (II). There is just a hint that some of the large deviations may be real and attributable to molecular-packing effects (see later).

The angular deviations just mentioned involve mainly lateral displacements (of up to 0·05 Å) of the H atoms in the ring planes. The displacements perpendicular to the ring planes are shown in Table 6. Of the 20 displacements, five have magnitudes >0·05 Å (~2·5σ) and all five are positive, *i.e.* towards the Fe atom of the molecule concerned. The mean displacement is +0·018 Å. As with the lateral distortions, there are hints from the packing analysis that some of the larger out-of-plane deformations may not be entirely spurious.

Table 4. *Bond distances* (Å) *from the* 101 K *analysis*

Values in parentheses are corrected for librational motion. E.s.d.'s are about 0·0015 Å for Fe–C, 0·002 Å for C–C and 0·02 Å for C–H.

	Molecule (I)	Molecule (II)
Fe–C(1)	2·043 (2·050)	2·041 (2·047)
Fe–C(2)	2·038 (2·045)	2·045 (2·050)
Fe–C(3)	2·046 (2·051)	2·052 (2·057)
Fe–C(4)	2·051 (2·055)	2·048 (2·055)
Fe–C(5)	2·049 (2·055)	2·046 (2·053)
Fe–C(6)	2·048 (2·053)	2·044 (2·049)
Fe–C(7)	2·048 (2·053)	2·042 (2·049)
Fe–C(8)	2·048 (2·055)	2·045 (2·053)
Fe–C(9)	2·045 (2·052)	2·048 (2·054)
Fe–C(10)	2·050 (2·056)	2·046 (2·051)
C(1)–C(2)	1·424 (1·431)	1·425 (1·432)
C(2)–C(3)	1·427 (1·434)	1·429 (1·436)
C(3)–C(4)	1·419 (1·427)	1·423 (1·430)
C(4)–C(5)	1·425 (1·432)	1·424 (1·432)
C(5)–C(1)	1·425 (1·432)	1·428 (1·435)
C(6)–C(7)	1·421 (1·428)	1·422 (1·430)
C(7)–C(8)	1·430 (1·438)	1·424 (1·431)
C(8)–C(9)	1·426 (1·433)	1·429 (1·436)
C(9)–C(10)	1·425 (1·432)	1·429 (1·436)
C(10)–C(6)	1·431 (1·438)	1·427 (1·434)
Fe–C (mean)	2·047 (2·053)	2·046 (2·052)
C–C (mean)	1·425 (1·433)	1·426 (1·433)
C–H	0·963–1·044	0·953–1·070
C–H (mean)	1·000	0·993

Thermal-motion analysis

We have analysed the atomic vibrational tensors (excluding H atoms) obtained by refinement of the three data sets collected at 101, 123 and 148 K. For this purpose we used the computer program *THMB* (Trueblood, 1978), which includes optional calculation of the quantities $\Delta_{A,B} = z^2_{A,B} - z^2_{B,A}$ along any interatomic vector AB ($z^2_{A,B}$ is here the mean-square

Table 5. CCH *bond angles* (°) *from the* 101 K *analysis*

E.s.d.'s are 1·4–1·6°. All CCC angles are 108 ± 0·5°.

	Molecule (I)	Molecule (II)
C(5)C(1)H(1)	126·3	125·2
C(2)C(1)H(1)	125·6	126·8
C(1)C(2)H(2)	126·2	124·3
C(3)C(2)H(2)	125·7	127·5
C(2)C(3)H(3)	126·0	124·0
C(4)C(3)H(3)	125·8	128·3
C(3)C(4)H(4)	125·6	125·0
C(5)C(4)H(4)	126·0	126·5
C(4)C(5)H(5)	126·8	127·0
C(1)C(5)H(5)	125·4	125·2
C(10)C(6)H(6)	125·6	125·5
C(7)C(6)H(6)	126·3	126·6
C(6)C(7)H(7)	125·6	128·0
C(8)C(7)H(7)	126·2	123·5
C(7)C(8)H(8)	125·8	123·8
C(9)C(8)H(8)	126·4	128·3
C(8)C(9)H(9)	127·2	126·4
C(10)C(9)H(9)	124·5	125·7
C(9)C(10)H(10)	126·6	128·5
C(6)C(10)H(10)	125·4	123·2

vibration amplitude of atom A in the direction of atom B). According to Hirshfeld's (1976) rigid-bond postulate, $\Delta_{A,B} \sim 0$ for bonded pairs of atoms of comparable mass, and in a rigid molecule this near equality should hold about as well for the non-bonded interatomic vectors as for the bonded ones (Rosenfield, Trueblood & Dunitz, 1978). Gross violations of the near equality for bonded pairs are indications that the atomic-vibration tensors derived from least-squares refinement are contaminated by experimental errors in the F values or by charge deformation densities or by disorder, or by combinations of these. On the other hand, if the near equality holds reasonably well (to within say 0·0010 Å^2) for bonded pairs but not for non-bonded pairs, this may indicate that the rigid-molecule approximation is not appropriate for analysing the thermal motion. Although $\Delta_{A,B} \sim 0$ is a necessary condition for the validity of the rigid-body model it is by no means sufficient since $\Delta_{A,B}$ is unaffected by vibration components perpendicular to the AB direction.

As an example, we may consider the $\Delta_{A,B}$ values for molecule (I) at 101 K (Table 7). The r.m.s. values of $\Delta_{A,B}$ are 0·0005 Å^2 for the ten bonded pairs of C atoms, 0·0009 Å^2 for the ten ring-diagonals, and 0·0011 Å^2 for the 20 inter-ring vectors. Since the e.s.d.'s in $\Delta_{C,C}$ are about 0·0010 Å^2 the near-equality condition is satisfied for both bonded and non-bonded C,C pairs as well as can be expected. At the higher temperatures the general increase in values of $\sigma(U^{ij})$, and hence of $\sigma(\Delta_{C,C})$, makes it difficult to draw any conclusions about the rigidity or non-rigidity of the C framework.

At 101 K the ten $\Delta_{Fe,C}$ values are all negative with a mean of −0·0034 (6) Å^2. In other words, the vibration components of the C atoms along the Fe—C directions are consistently larger than those of the Fe atom, indicating that the C-atom framework is vibrating as a whole relative to the Fe atom. Very similar results are obtained for molecule (II), where the mean value of $\Delta_{Fe,C}$ is −0·0032 (4) Å^2. Independent estimates of the mean vibration amplitudes in ferrocene are available from gas-phase electron diffraction studies (Haaland & Nilsson, 1968) and from calculations based on a harmonic force field derived from vibrational frequencies (Schäfer, Brunvoll & Cyvin, 1972). From electron diffraction the mean-square vibration amplitude along the Fe···C direction is 0·0038 Å^2 at 413 K, while the calculations yield values of 0·0055 Å^2 at 298 K and 0·0035 Å^2 at 0 K. Our values of 0·0035 Å^2 (molecule I) and 0·0032 Å^2 (molecule II) at 101 K refer to the mean-square amplitude of the C-atom framework relative to the Fe atom, but the motion of the latter can be neglected in first approximation.

The $\Delta_{Fe,C}$ values at the two higher temperatures show much the same behaviour; all are negative, as at 101 K, with mean values of −0·0026 (7) and −0·0030 (14) Å^2 for molecule (I) and of −0·0022 (8) and −0·0023 (10) Å^2 for molecule (II) at 123 and 148 K respectively.

For the thermal-motion-analysis calculations (Schomaker & Trueblood, 1968) we assume the molecule to be rigid at all three temperatures and we also include the vibration tensor of the central Fe atom. The

Table 6. *Displacements* (Å) *of* H *atoms from mean planes of the cyclopentadienyl* C *skeletons*

The ring skeletons themselves are planar to within 0·002 Å and the e.s.d.'s in H positions are about 0·02 Å. A positive sign indicates that the displacement is towards the Fe atom.

	Molecule (I)		Molecule (II)	
H(1)	−0·023		+0·016	
H(2)	+0·075		+0·001	
H(3)	+0·093		+0·031	
H(4)	−0·003		+0·017	
H(5)	−0·015		−0·016	
H(6)		+0·035		+0·008
H(7)		−0·032		+0·060
H(8)		−0·035		+0·022
H(9)		−0·029		+0·021
H(10)		+0·066		+0·070

Table 7. *Values of* $\Delta_{A,B} = z^2_{A,B} - z^2_{B,A}$ *in* Å^2 × 10^4 *for all atom pairs* (*excluding* H *atoms*) *in molecule* (I) *at* 101 K

Bonds are indicated by bold face. E.s.d.'s are about 7 units in $\Delta_{Fe,C}$ and about 10 units in $\Delta_{C,C}$.

	B	Fe	C(1)	C(2)	C(3)	C(4)	C(5)	C(6)	C(7)	C(8)	C(9)	C(10)
A												
Fe		.	−24	−41	−37	−27	−42	−39	−31	−29	−41	−28
C(1)			.	**+2**	+3	−13	**+9**	−21	+4	+3	−12	+14
C(2)				.	**0**	−5	+17	+6	−4	+14	−5	+20
C(3)					.	**+3**	+2	−2	0	+6	0	+6
C(4)						.	**−3**	−8	−6	−4	−6	−2
C(5)							.	−5	+14	+13	+17	+7
C(6)								.	**0**	+11	−4	**−3**
C(7)									.	**+2**	−5	+4
C(8)										.	**+2**	+8
C(9)											.	**−11**
C(10)												.

Table 8. *Results of rigid-body-motion analysis*

Because of the approximate D_5 symmetry, two eigenvalues of the inertial tensor are nearly equal and the corresponding eigenvectors are sensitive to very small changes in the atomic positions. The inertial system is therefore not suitable for comparing results at different temperatures. In its place we refer all vectors to a set of Cartesian axes along **a**, **c*** × **a**, **c***. The translation tensor **T** is given in its reduced form (Schomaker & Trueblood, 1968). R' is $[\sum(\Delta U)^2/\sum U^2]^{1/2}$.

	101 K				123 K				148 K			
	Eigenvalue	Eigenvector			Eigenvalue	Eigenvector			Eigenvalue	Eigenvector		
Molecule (I)												
Fivefold axis		0·6958	0·7164	0·0518		0·6953	0·7168	0·0523		0·6952	0·7167	0·0547
L_1 (deg²)	28·22	0·8177	0·5747	0·0329	42·76	0·8026	0·5954	0·0366	58·30	0·8064	0·5890	0·0521
L_2 (deg²)	5·39	−0·1166	0·2213	−0·9682	6·63	−0·1516	0·2628	−0·9529	8·46	−0·0505	0·1564	−0·9864
L_3 (deg²)	5·00	−0·5637	0·7879	0·2480	6·22	−0·5770	0·7592	0·3012	6·89	−0·5892	0·7929	0·1558
T_1 (10^{-4} Å²)	140	0·1642	0·2956	−0·9411	163	0·1132	0·3081	−0·9446	213	0·1731	0·2166	−0·9608
T_2 (10^{-4} Å²)	115	−0·9862	0·0685	−0·1506	140	−0·9143	0·4045	0·0224	175	−0·9665	0·2251	−0·1234
T_3 (10^{-4} Å²)	100	0·0200	0·9528	0·3028	112	0·3890	0·8611	0·3275	134	0·1896	0·9500	0·2483
$\langle\Delta U^2\rangle^{1/2}$ (Å²)		12×10^{-4}				16×10^{-4}				27×10^{-4}		
R'		0·070				0·078				0·099		
Molecule (II)												
Fivefold axis		0·6774	−0·7322	0·0711		0·6793	−0·7306	0·0700		0·6819	−0·7283	0·0682
L_1 (deg²)	28·59	0·6953	0·7072	−0·1279	41·89	0·6914	−0·7157	−0·0981	55·36	0·6973	−0·7103	−0·0956
L_2 (deg²)	6·79	0·7068	0·6406	0·3000	8·28	0·7165	0·6620	0·2202	10·23	0·7102	0·6668	0·2260
L_3 (deg²)	4·47	−0·1302	−0·2990	0·9453	4·99	−0·0927	−0·2226	0·9705	5·77	−0·0968	−0·2255	0·9694
T_1 (10^{-4} Å²)	143	0·1079	0·0886	−0·9902	167	−0·3310	−0·4913	−0·8056	212	0·1246	−0·0742	−0·9894
T_2 (10^{-4} Å²)	130	0·6752	0·7246	0·1384	161	0·6278	0·5228	−0·5768	203	0·7168	0·6962	0·0380
T_3 (10^{-4} Å²)	101	0·7297	−0·6835	0·0184	107	0·7045	−0·6966	0·1354	130	0·6860	−0·7140	0·1400
$\langle\Delta U^2\rangle^{1/2}$ (Å²)		10×10^{-4}				14×10^{-4}				20×10^{-4}		
R'		0·059				0·068				0·075		

Table 9. *Displacements* (Å) *of libration axes from the molecular centre, measured parallel to the principal axes L_1, L_2, L_3 of the libration tensor in each case*

For molecule (I), positive L_1 runs towards ring C(6)–C(10), for molecule (II) towards ring C(1)–C(5).

	Molecule (I)			Molecule (II)		
	L_1	L_2	L_3	L_1	L_2	L_3
101 K						
$\rho(L_1)$	0	−0·360	0·303	0	−0·305	−0·301
$\rho(L_2)$	0·324	0	−0·245	−0·069	0	−0·349
$\rho(L_3)$	0·559	−0·199	0	0·384	0·224	0
123 K						
$\rho(L_1)$	0	−0·310	0·241	0	−0·273	−0·292
$\rho(L_2)$	0·311	0	−0·330	−0·022	0	−0·258
$\rho(L_3)$	0·618	−0·211	0	0·314	0·463	0
148 K						
$\rho(L_1)$	0	−0·298	0·293	0	−0·325	−0·277
$\rho(L_2)$	0·382	0	−0·199	−0·055	0	−0·261
$\rho(L_3)$	0·820	−0·287	0	0·321	0·558	0

assumption of rigid-body motion is a very questionable one for ferrocene. From electron diffraction studies (Haaland & Nilsson, 1968) the barrier to internal rotation of the cyclopentadienyl rings in the free molecule is $<4{\cdot}2$ kJ mol^{-1}. Furthermore, as discussed above, the relative motion of the C-atom framework with respect to the Fe atom can be detected from analysis of the vibration amplitudes along the Fe–C directions in the crystal. On the other hand, the rigid-body model has the advantage of simplicity and leads to the most concise possible description of the correlations among the individual atomic vibration tensors. Despite its obvious deficiencies the rigid-body model turns out to give reasonably good agreement between calculated and observed U^{ij} values. To some extent, these deficiencies are simply absorbed in the adjustable parameters.

For example, the relative motion of the C-atom framework with respect to the Fe atom is absorbed in the translation tensor component parallel to the molecular symmetry axis. Slightly better numerical agreement between observed and calculated C-atom vibration components in this direction would have been obtained by omitting the Fe atoms from the thermal-motion calculations. These atoms, however, provide important information about the other translation components, and this information would be lost if the Fe contributions were omitted altogether. As a compromise, we have included Fe and C contributions with equal weights. In any case, this uncertainty in the correct choice of weights does not affect the calculation of the libration tensor, in which we are mainly interested.

The main results of the thermal-motion analysis are summarized in Table 8. With allowance for the non-optimal weighting scheme, the agreement obtained between observed and calculated U^{ij} values is about as good as can be expected from the experimental uncertainties. Thus the rigid-body model would seem to be compatible with the observed U^{ij} values, even if it is not strictly valid according to the other tests mentioned earlier. Also, it is clear that information about mean-

square vibration amplitudes cannot distinguish between in-phase libration of the rings (rigid-body rotation) and out-of-phase libration (internal motion).

Table 8 indicates that the principal libration axis L_1 is in all cases nearly parallel to the molecular fivefold axis. Reduction of the **T** tensor in terms of the non-intersecting-axes description (Schomaker & Trueblood, 1968) shows, however, that L_1 does not pass through the molecular centre. Neither do the other libration axes L_2 and L_3. The calculated displacements (Table 9) are quite similar at the three temperatures, except that with increasing temperature, L_3 of molecule (I) is displaced more and more towards ring C(6)–C(10). The displacement of L_1 from the molecular centre amounts to 0·4–0·45 Å for both molecules; its direction is roughly towards C(4) in molecule (I) and away from C(2) in molecule (II). The absence of fivefold symmetry of the vibration ellipsoids in a given ring (Fig. 1) is connected with these libration-axis displacements (and also with the differences between the eigenvalues along L_2 and L_3).

The largest eigenvalues of the libration tensors of the two molecules are nearly equal and show a practically linear temperature dependence (Fig. 2). In their study of the libration of 9,10-anthraquinone at five temperatures, Shmueli & Kroon (1974) have shown that the observed libration amplitudes are reasonably well reproduced by the relationship $\langle\varphi^2\rangle = RT/k$, where k is the effective force constant associated with the motion. The value of k at each temperature was estimated by calculating the energy increments associated with displacement of the molecule from equilibrium. In agreement with quasi-harmonic theory (Willis, 1969; Willis & Pryor, 1976) the effective force constants become smaller with increase in temperature. From our results, the energy increase associated with displacement from equilibrium can be estimated to be about 29, 24 and 22 J mol^{-1} deg^{-2} for the L_1 libration at 101, 123 and 148 K respectively, and about 145–170 J mol^{-1} deg^{-2} for the L_2 and L_3 librations with a much smaller temperature dependence. Extrapolation of the L_1 *versus* T curve yields a libration amplitude of about 8° (approximately equal to the rotation angle between the rings in the equilibrium structure) at the transition temperature of 164 K.

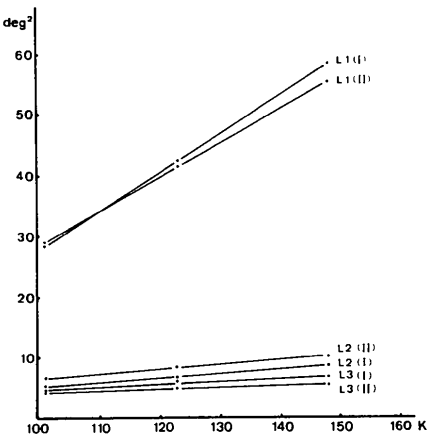

Fig. 2. Temperature dependence of the eigenvalues L_1, L_2, L_3 of the libration tensor **L** for molecules (I) and (II).

In an alternative model, the two C-atom rings in each molecule could have been treated as separate rigid bodies and each allowed to vibrate independently of the other. However, the five C atoms of each ring lie almost exactly on a circle, leading to a singularity in the matrix of normal equations (Cruickshank, 1956) if the rings are treated separately. In any case, if the librational motion of the two rings in a given molecule were very different, the rigid-molecule model would lead to a systematic overestimation of the vibration amplitudes in one ring and an underestimation in the other. For molecule (I), a slight tendency in this direction is just detectable, suggesting that the vibrational amplitude about the fivefold axis may be 5–10% greater for ring C(1)–C(5) than for ring C(6)–C(10).

Crystal packing

With two symmetry-independent (but virtually D_5 symmetric) molecules in the asymmetric unit of the crystal, a detailed verbal description of the packing becomes rather complicated. A stereopicture of a complete unit cell, viewed along a direction slightly tilted to **b**, is shown in Fig. 3; here the label *G* denotes the reference molecule of type (I) whose coordinates

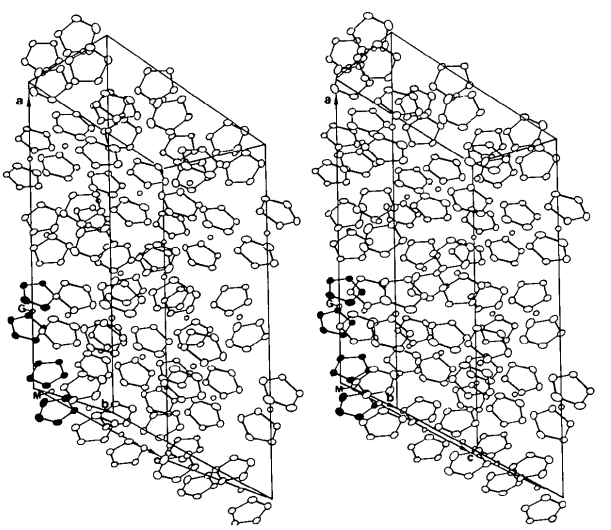

Fig. 3. Stereoscopic view of the low-temperature triclinic unit cell of ferrocene. The letters *G* and *M* refer to the reference molecules of types (I) and (II) respectively whose coordinates are listed in Table 2.

are listed in Table 1, while label *M* denotes the corresponding reference molecule of type (II). For clarity, H atoms are omitted in Fig. 3, but they are included in Figs. 4 and 5, which show the contacts made by molecules *G* and *M* with neighbouring molecules. The actual H···H intermolecular distances are uncertain because we do not know exactly where to place the H atoms. Besides their inherent inaccuracy, the observed positions are systematically displaced towards the C atoms (the mean C–H distance of 1·00 Å is about 0·08 Å too short). On the other hand, the idealized H-atom positions, calculated on the assumption that the H atoms of each cyclopentadienyl moiety are symmetrically disposed in the ring plane with C–H = 1·08 Å, lead to intermolecular H···H distances as short as 2·23 Å. While still shorter H···H distances are known to occur in constrained situations (Ermer, Dunitz & Bernal, 1973), the short distances calculated from idealized positions must at least be regarded with some suspicion. It is suggestive that the corresponding H···H distances calculated from the observed H positions include no such suspicious features (Table 10).

Molecule *G* (type I) is effectively in close packing with its neighbours. It is in contact with 12 surrounding molecules (marked *A–F*, *H–M* in Fig. 4) with 25 intermolecular H···H distances <2·8 Å [nine such distances <2·5 Å (idealized positions) are indicated in Fig. 4]. Molecule *M* (type II) is in contact with 11 surrounding molecules (*G*, *H*, *J*, *K*, *L*, *N–S*) with 23 intermolecular H···H distances <2·8 Å (11 such distances <2·5 Å are indicated in Fig. 5). The five shortest intermolecular contact distances (2·23, 2·24, 2·30, 2·32, 2·34 Å based on idealized positions) are all between molecules of different type. There are also several short intermolecular C···H distances in the range 2·73–2·80 Å, also between molecules of different type.

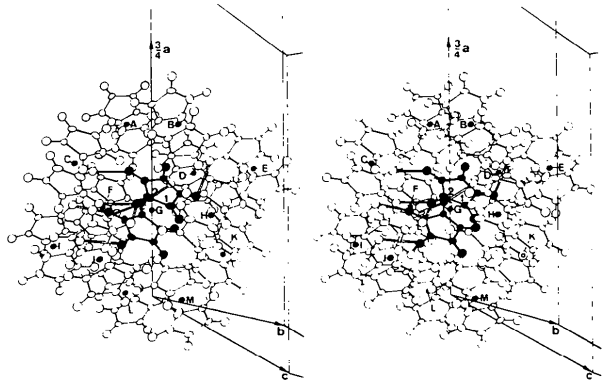

Fig. 4. Stereoscopic view of reference molecule *G* (type I) and its nearest neighbours.

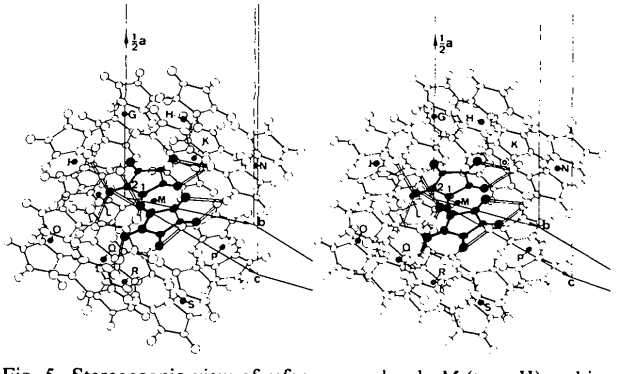

Fig. 5. Stereoscopic view of reference molecule *M* (type II) and its nearest neighbours.

Table 10. *Intermolecular* H···H *distances calculated from observed and idealized* (*in parentheses*) H *positions*

The individual molecules denoted by capital letters in Figs. 4 and 5 are related to the reference molecules (I) and (II) as follows:

A	54503 (II)	*G*	55501 (I)	*M*	55501 (II)	*S*	45503 (I)
B	55504 (II)	*H*	55504 (I)	*N*	55507 (I)		
C	55406 (I)	*I*	55407 (II)	*O*	45405 (I)		
D	55506 (II)	*J*	55408 (II)	*P*	55508 (II)		
E	55505 (II)	*K*	55506 (I)	*Q*	55408 (I)		
F	54504 (I)	*L*	55502 (II)	*R*	55502 (I)		

where the last digit specifies a given equivalent position:

(1)	x,y,z	(5)	$\frac{1}{2}+x, y, \frac{1}{2}+z$
(2)	$-x,-y,-z$	(6)	$\frac{1}{2}-x,-y,\frac{1}{2}-z$
(3)	$\frac{1}{2}+x,\frac{1}{2}+y,z$	(7)	$x,\frac{1}{2}+y,\frac{1}{2}+z$
(4)	$\frac{1}{2}-x,\frac{1}{2}-y,z$	(8)	$-x,\frac{1}{2}-y,\frac{1}{2}-z$

and translations along **a**,**b**,**c** add or subtract one from the first three digits, which are 555 for the two standard molecules *G* and *M*.

G Type (I)	Neighbour *A*	*M*	*T**	*d* (Å)	*M* Type (II)	Neighbour *A*	*M*	*T**	*d* (Å)
1	1	*H*	(I)	2·59 (2·58)	1	1	*L*	(II)	2·52 (2·48)
	4	*M*	(II)	2·68 (2·60)		6	*R*	(I)	2·72 (2·66)
2	7	*J*	(II)	2·35 (2·23)	2	5	*O*	(I)	2·34 (2·30)
	3	*C*	(I)	2·48 (2·50)		8	*J*	(II)	2·57 (2·43)
3	2	*C*	(I)	2·48 (2·50)	3	8	*J*	(II)	2·58 (2·56)
	3	*C*	(I)	2·65 (2·71)		7	*J*	(II)	2·77 (2·69)
	9	*B*	(II)	2·74 (2·59)	4	8	*N*	(I)	2·40 (2·32)
	8	*C*	(I)	2·75 (2·63)		1	*G*	(I)	2·68 (2·60)
4	5	*D*	(II)	2·72 (2·63)	5	9	*K*	(I)	2·38 (2·24)
5	2	*E*	(II)	2·34 (2·30)		10	*P*	(II)	2·64 (2·55)
	10	*K*	(I)	2·62 (2·52)		4	*K*	(I)	2·72 (2·63)
	6	*K*	(I)	2·71 (2·57)	6	10	*P*	(II)	2·56 (2·48)
6	10	*K*	(I)	2·59 (2·56)		9	*S*	(I)	2·70 (2·55)
	5	*K*	(I)	2·71 (2·57)	7	2	*Q*	(I)	2·35 (2·23)
	1	*L*	(II)	2·72 (2·66)		3	*J*	(II)	2·77 (2·69)
7	8	*J*	(II)	2·53 (2·34)	8	7	*Q*	(I)	2·53 (2·34)
	9	*I*	(II)	2·57 (2·48)		2	*J*	(II)	2·57 (2·43)
8	4	*I*	(II)	2·40 (2·32)		3	*J*	(II)	2·58 (2·56)
	3	*C*	(I)	2·75 (2·63)	9	7	*N*	(I)	2·57 (2·48)
9	5	*D*	(II)	2·38 (2·24)		3	*H*	(I)	2·74 (2·59)
	9	*F*	(I)	2·43 (2·42)	10	10	*P*	(II)	2·52 (2·62)
	6	*A*	(II)	2·70 (2·55)		6	*P*	(II)	2·56 (2·48)
10	6	*K*	(I)	2·59 (2·56)		5	*P*	(II)	2·64 (2·55)
	5	*K*	(I)	2·62 (2·52)					
	10	*K*	(I)	2·75 (2·82)					

* *A* = atom, *M* = molecule, *T* = type.

The ferrocene molecules in the LT crystal are neither eclipsed nor staggered but closer to the former. The deviation from eclipsing increases slightly between 101 and 148 K. The barrier to internal rotation in the free molecule is expected to be quite small, so it seems likely that the observed conformations are largely determined by packing forces. This seems to be confirmed by preliminary calculations of the dependence of the crystal-packing energy on the orientation of individual C_5H_5 rings (Maverick, unpublished results).

Difference syntheses

Sections of an $(F_o - F_c)$ synthesis for the 101 K data are shown in Fig. 6. The F_c values used for this calculation are not quite the same as those obtained from the structural model defined by the parameters in Table 1. In order to counteract the systematic shortening of the C–H bonds, the H atoms were moved from their observed positions along the C–H directions to make all C–H distances equal to 1·08 Å. Least-squares refinement with fixed H positions was then carried out [isotropic thermal parameters for H atoms, modified weighting scheme (Dunitz & Seiler, 1973) with $r = 5$ Å^2], leading to slight changes in the vibrational parameters of the C atoms, but not in their positions. R obtained in this constrained refinement was 0·021 (compare with 0·019 for parameters of Table 1). The e.s.d. of residual density in the $(F_o - F_c)$ synthesis is 0·05 e Å^{-3}. The observed densities at the Fe positions are zero within 0·1 e Å^{-3}.

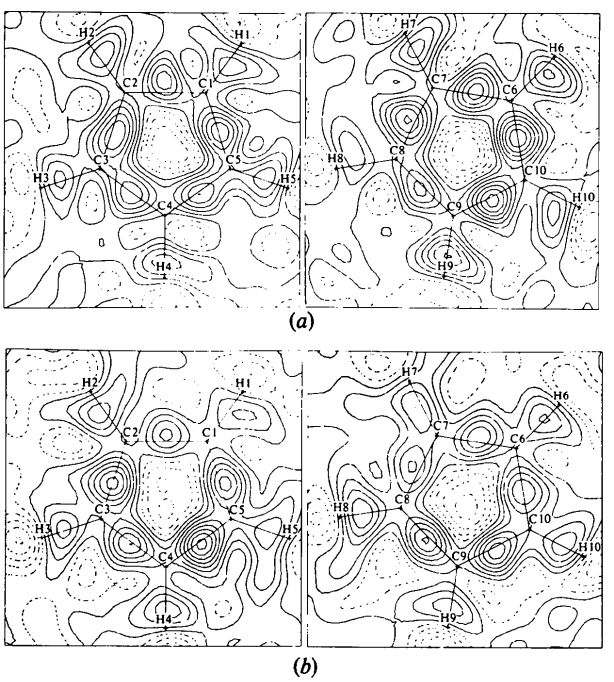

Fig. 6. X–X deformation maps (101 K data) in the planes of the four symmetry-independent cyclopentadienyl rings. (*a*) Molecule (I), (*b*) molecule (II). Contour lines are drawn at intervals of 0·05 e Å^{-3}, negative contour lines being broken.

Apart from a somewhat ill defined band of density round each Fe atom, the main features of the difference synthesis are the residual electron density peaks of 0·15–0·3 e Å^{-3} at or near the midpoints of the C–C and C–H bonds. The C–H peaks would have been much less prominent if the calculation had been based on observed H positions, and the C–C peaks would have been less prominent if the structural model had included higher-order terms in the description of the thermal motion. In fact, the residual electron density peaks at the midpoints of the C–C bonds are extremely sensitive to the thermal-motion assumptions in the structural model. For example, when the difference map is recalculated with F_c values based on isotropic temperature factors for the C atoms, the residual peaks at the midpoints of the C–C bonds amount to 0·8–1·3 e Å^{-3}. (In evaluating the significance of these residual peaks it should be kept in mind that the electron density peaks in the F_o synthesis have heights of about 12 e Å^{-3} for C and about 100 e Å^{-3} for Fe atoms.)

Although the deformation density (change in electron density distribution from free atoms on molecule formation) for each C_5H_5 fragment can be expected to have virtually perfect fivefold symmetry, the deviations from fivefold symmetry in the 101 K difference map are unmistakable. These deviations are only partly due to experimental errors in the F_o values; they also arise from the absence of fivefold symmetry in the thermal ellipsoids.

It appears that in order to be able to interpret the residual density in the $(F_o - F_c)$ synthesis as genuine deformation density, it would have been necessary to measure the F_o values at a temperature lower than 100 K, at a temperature where the librational disorder of the C_5H_5 rings is effectively frozen out. Fig. 2 suggests that cooling to below 70 K would have been necessary for this purpose. Although no direct comparison is possible, it is interesting to note that the recent X-ray and neutron diffraction study of bis[dicarbonyl(η-cyclopentadienyl)iron], $[(C_5H_5)Fe(CO)_2]$, by Mitschler, Rees & Lehmann (1978) indicates that libration of the C_5H_5 ring in this crystal is still not entirely frozen out even at 70 K.

The choice of space group

Although our initial assumption of space group $F\bar{1}$ seems to be rather well satisfied by the course of the subsequent structure analysis, we cannot entirely exclude the possibility that the centre of inversion and/or the F-centring are only approximate. If this were the case, then each of the two independent mol-

ecules in our assumed asymmetric unit would actually have to be regarded as an averaged superposition of two or more molecules displaced from the positions and orientations they would have in the reported structure. Any such displacement must be small for the Fe atoms but not necessarily for the light atoms, where the deviations from fivefold symmetry in the vibrational ellipsoids of the C atoms could be interpreted just as well in terms of a superposition model as by the thermal-motion analysis described earlier in this paper. The interpretation in terms of superposition structures would have to follow along much the same lines as that provided for the high-temperature phase (Seiler & Dunitz, 1979).

We made one attempt to refine the structure in the noncentrosymmetric space group $F1$ by full-matrix least squares (101 K, modified weighting scheme, small shifts applied to atomic positions to generate starting structure, all atoms considered as isotropic with U values of related pairs of atoms constrained to be equal, H atoms omitted). This analysis led to $R = 0{\cdot}050$, quite comparable to that obtained for the centrosymmetric structure with isotropic Fe and C and omitting H atoms. The noncentrosymmetric refinement led, of course, to a much less regular molecular geometry because of the ill-conditioning of the least-squares normal equations that must occur for a closely centrosymmetric structure (Ermer & Dunitz, 1970). Several other attempts were made to refine in the lower space group using other types of constraint, but all were as inconclusive as the first.

We must conclude that with the 101 K data it is virtually impossible to decide to what extent the irregular behaviour of the thermal ellipsoids is due to genuine thermal motion or to the assumption of only two molecules in the asymmetric unit. In this connexion, it is interesting that ESR measurements at liquid-He temperature of ferrocene doped with cobaltocene show the presence of at least two (and possibly more) types of molecular site with closely similar magnetic properties (Bucher, 1977; Ammeter, 1978).

In retrospect, it would appear that an X-ray analysis of ferrocene at a lower temperature than 100 K would be necessary to answer some of these questions.

We thank Professor K. N. Trueblood for helpful comments on the manuscript.

References

AMMETER, J. H. (1978). *J. Magn. Reson.* **30**, 299–325.

BODENHEIMER, J. S. & LOW, W. (1971). *Phys. Lett. A*, **36**, 253–254.

BUCHER, R. (1977). Dissertation No. 5946. ETH Zürich.

CALVARIN, G. & BÉRAR, J. F. (1975). *J. Appl. Cryst.* **8**, 380–385.

CRUICKSHANK, D. W. J. (1956). *Acta Cryst.* **9**, 754–756.

DUNITZ, J. D. & ORGEL, L. E. (1953). *Nature (London)*, **171**, 121–122.

DUNITZ, J. D., ORGEL, L. E. & RICH, A. (1956). *Acta Cryst.* **9**, 373–375.

DUNITZ, J. D. & SEILER, P. (1973). *Acta Cryst.* B**29**, 589–595.

EDWARDS, J. W. & KINGTON, G. L. (1962). *Trans. Faraday Soc.* **58**, 1323–1333.

EDWARDS, J. W., KINGTON, G. L. & MASON, R. (1960). *Trans. Faraday Soc.* **56**, 660–667.

ERMER, O. & DUNITZ, J. D. (1970). *Acta Cryst.* A**26**, 163.

ERMER, O., DUNITZ, J. D. & BERNAL, I. (1973). *Acta Cryst.* B**29**, 2278–2285.

HAALAND, A. (1975). *Top. Curr. Chem.* **53**, 1–23.

HAALAND, A. & NILSSON, J. E. (1968). *Acta Chem. Scand.* **22**, 2653–2670.

HIRSHFELD, F. L. (1976). *Acta Cryst.* A**32**, 239–244.

International Tables for X-ray Crystallography (1968). Vol. III, 2nd ed., Table 3.3.1A. Birmingham: Kynoch Press.

JOHNSON, C. K. (1965). *ORTEP*. Report ORNL-3794. Oak Ridge National Laboratory, Tennessee.

MITSCHLER, A., REES, B. & LEHMANN, M. S. (1978). *J. Am. Chem. Soc.* **100**, 3390–3397.

ROSENFIELD, R. E., TRUEBLOOD, K. N. & DUNITZ, J. D. (1978). *Acta Cryst.* A**34**, 828–829.

SCHÄFER, L., BRUNVOLL, J. & CYVIN, S. J. (1972). *J. Mol. Struct.* **11**, 459–474.

SCHOMAKER, V. & TRUEBLOOD, K. N. (1968). *Acta Cryst.* B**24**, 63–76.

SEILER, P. & DUNITZ, J. D. (1979). *Acta Cryst.* B**35**, 1068–1074.

SHMUELI, U. & KROON, P. A. (1974). *Acta Cryst.* A**30**, 768–771.

TAKUSAGAWA, F. & KOETZLE, T. F. (1979). *Acta Cryst.* B**35**, 1074–1081.

TRUEBLOOD, K. N. (1978). *Acta Cryst.* A**34**, 950–954.

WILLIS, B. T. M. (1969). *Acta Cryst.* A**25**, 277–300.

WILLIS, B. T. M. & PRYOR, A. W. (1976). *Thermal Vibrations in Crystallography*. Cambridge Univ. Press.